ISSN: 3033-3652

Journal of Physical Mathematics & its Applications

SCIENTIFIC Research and Community

Review Article

Open Access

Killing Magnetic Curves in 3-Dimension Heisenberg Group

Xinyu Bian and Yanhua Yu*

Department of Mathematics, Northeastern University, Shenyang, 110819, PR China

ABSTRACT

In this paper, we derive the equations governing the magnetic trajectories produced by Killing vector fields in 3-dimension Heisenberg group, denoted as *H*3. Given the challenges in obtaining analytical solutions for these Killing magnetic curves, we resort to the perturbation method to ascertain approximate solutions. To enhance the accuracy of these approximates, we utilize three distinct techniques: the straightforward perturbation method, the *Lindstedt – Poincare´* method, and the homotopy perturbation method. Subsequently, we visually compare these approximated solutions with numerical solutions through graphical representations. Ultimately, our findings reveal that the homotopy perturbation method yields the most precise approximation among the three aforementioned methods.

***Corresponding author**

Yanhua Yu, Department of Mathematics, Northeastern University Shenyang, 110819, PR China.

Received: March 11, 2025; **Accepted:** March 17, 2025; **Published:** March 24, 2025

Keywords: Killing Magnetic Curves, Heisenberg Group, Straightforward Perturbation Method, Lindstedt − Poincare´ Method, Homotopy Perturbation Method

Introduction

The investigation of the Killing magnetic curve serves as a pivotal cornerstone for the advancement of electromagnetic technology, significantly enhancing technological sophistication and fostering the integration of novel materials. Neves et al. contributed notably by refining the magnetic attributed and dye removal efficiency of composite materials through a meticulous analysis of magnetic force curves. Their adjustments to the composition and structure of these materials facilitated optimized application in environmental governance [1]. Farzin et al. leveraged magnetic force curves to assess the magnetic properties of nanoparticles, enabling the design of specific nanoparticles configurations with tailored magnetic characteristics. This research led to more effective strategies for cancer diagnosis and treatment [2].

Over the past two decades, research into magnetic curves across diverse geometric structures has grown significantly. Bejan et al. have offered several classifications of magnetic curves on Para-Sasakian manifolds [3]. Calvaruso delved into examples within the hyperbolic Heisenberg group and other three-dimensional almost para- contact manifolds [4]. Munteanu et al. contributed by classifying magnetic trajectories that are Frenet curves of maximum order 5 within the Heisenberg group $H(n, 1)$ of dimension $(2n + 1)$ [5]. Furthermore, Korpinar et al. investigated B⌊-magnetic curves in three-dimensional Riemannian manifold, providing valuable insights as outlined in [6]. Lee explored contact magnetic curves in Sasakian Lorentzian 3- manifolds, enriching our comprehension as presented in [7]. The Killing magnetic curves in $SL(2, \mathbb{R})$ geometry has been studied by Erjavec [8]. Inoguchi and Munteanu investigated magnetic curves in Killing submersions [9]. Additionally, Sun recon- $\mathbb{R}^3_1$cted the Cartan Equations for null Killing magnetic curve in R3 with Killing magnetic vector field [10].

Kelekci employed the perturbation method, up to the first order, to tackle the intricate problem of trajectories generated by Killing vector fields within Hyperbolic spaces, as documented in his work [11]. Perturbation methods have found extensive application across diverse academic disciplines for analyzing nonlinear systems. Nayfeh provided a comprehensive introduction to the fundamental principles and techniques of straightforward perturbation theory, with a particular emphasis on the analysis of nonlinear problems, in his seminal work [12]. Furthermore, to ad- dress the nonlinear dependency of frequency on nonlinearity, he introduced the Lindstedt-Poincare method. However, in scenarios where equations lack parameters, both the straightforward perturbation method and the Lindstedt-Poincare method encounter limitations. To overcome these challenges, Ji-Huan He explored the homotopy perturbation method, leveraging the construction of a homotopy equation that incorporates perturbation parameters, to solve a range of complex nonlinear problems [13].

Drawing inspiration from the aforementioned insights, our objective is to delve into the exploration of the Killing magnetic force curve within the Heisenberg group. This particular choice is driven by the group's distinctive spatial symmetries, which facilitate a deeper and more nuanced analysis. Consequently, this endeavor holds profound implications for quantum mechanics and quantum field theory, with potential applications spanning general relativity and black hole physics, as evidenced in the works of [14,15]. With the aim of achieving more re- fined solutions, we undertake a comparative analysis of three distinct perturbation methods.

The structure of this paper is organized as follows: In Section 2, we present the fundamental geometric structure that will be utilized in the subsequent sections of the paper. In Section 3, we offer a comprehensive proof for the existence of the Killing vector field within the three-dimensional Heisenberg group, denoted as H3. Moving on to Section 4, we tackle the equation system associated with the Killing magnetic force curve on the Heisenberg group. To obtain more accurate approximation results, we calculate and compare three distinct perturbation methods: the straightforward perturbation method, the Lindstedt-Poincare method, and the homotopy perturbation method.

Preliminaries

In the realm of geometric physics, magnetic fields are frequently modeled utilizing the principles of contact geometry. Within this context, the magnetic field is regarded as a unique geometric phenomenon that manifests on a contact manifold. Here, the magnetic field serves as a constraint, influencing the dynamics of matter via the contact structure. In these theoretical frameworks, the magnetic field exerts an influence on the trajectories of particles traversing the manifold, and the nature of this motion is dictated by the contact structure. Notably, the Heisenberg group constitutes a contact manifold, as highlighted and its inherent contact structure offers avenues for deeper exploration and study [16].

It's evident that 3-dimensional Heisenberg group, denoted as (H_3, g, ϕ, ξ, η) possesses an almost contact structure. In which g is a metric, ϕ is a $(1, 1)$ −tensor field, ξ is a vector field, η 1−form contact structure, satisfying [17]

$$\phi^2 = -\mathrm{I} + \eta \otimes \xi, \eta(\xi) = 1,$$

and

$$\phi\xi = 0, \eta \circ \phi = 0.$$

In this scenario, a closed 2−form on H_3 gives rise to a magnetic field F, where the corresponding Lorentz force ϕ, associated with F, is defined as follows:

$$F(X_\imath, X_\jmath) = g(\phi X_\imath, X_\jmath), X_\imath, X_\jmath \in \mathfrak{X}(\mathcal{M}).$$

The smooth curve γ on H_3 is referred to as a magnetic curve for the magnetic field F if it serves as a solution to the Lorentz equation [18].

$$\nabla_{\dot{\gamma}}\dot{\gamma} = \phi(\dot{\gamma}).$$

Regarding F, if we wish to categorize it as a Killing vector field, it must satisfy the following Killing equation

$$\nabla_\mu F_\vartheta + \nabla_\vartheta F_\mu = 0.$$

The Heisenberg group H_3 can be seen as the space $\mathbb{R}^3$ endowed with the multiplication

$$(x', y', z')(x, y, z) = \left(x' + x, y' + y, z' + z + \frac{1}{2}x'y - \frac{1}{2}y'x\right).$$

and the Riemannian metric g given by

$$g = dx^2 + dy^2 + \left(dz + \frac{y}{2}dx - \frac{x}{2}dy\right)^2.$$

Firstly, we will determine the Levi-Civita connection ∇ of the metric g in relation to the left invariant orthonormal basis

$$e_1 = \frac{\partial}{\partial x} - \frac{y}{2}\frac{\partial}{\partial z},\ e_2 = \frac{\partial}{\partial y} + \frac{x}{2}\frac{\partial}{\partial z},\ e_3 = \frac{\partial}{\partial z}.$$

We can easily check that

$$\begin{aligned}
&\nabla_{e_1}e_1 = 0, && \nabla_{e_1}e_2 = \frac{1}{2}e_3, && \nabla_{e_1}e_3 = -\frac{1}{2}e_2,\\
&\nabla_{e_2}e_1 = -\frac{1}{2}e_3, && \nabla_{e_2}e_2 = 0, && \nabla_{e_2}e_3 = \frac{1}{2}e_1,\\
&\nabla_{e_3}e_1 = -\frac{1}{2}e_2, && \nabla_{e_3}e_2 = \frac{1}{2}e_1, && \nabla_{e_3}e_3 = 0.
\end{aligned}$$

In the meantime, we have the well-established Lie bracket relations

$$[e_1, e_2] = e_3,\ [e_3, e_1] = 0,\ [e_2, e_3] = 0.$$

Killing Vector Field in H_3

The research carried out by Rahmani explores Killing vector fields in Heisenberg group with the Lorentzian left invariant metric $g = -\mathrm{d}x^2 + \mathrm{d}y^2 + (x\mathrm{d}y + \mathrm{d}z)^2$ [19]. Consequently, we arrive at the following Lemma.

Lemma 1: *The Lie algebra of infinitesimal isometries of (H_3, g) is four- dimensional and admits as basis the following vector fields:*

$$\mathbb{X}_1 = y\frac{\partial}{\partial x} - x\frac{\partial}{\partial y},\ \mathbb{X}_2 = -\frac{\partial}{\partial y} + \frac{x}{2}\frac{\partial}{\partial z},\ \mathbb{X}_3 = \frac{\partial}{\partial x} + \frac{y}{2}\frac{\partial}{\partial z},\ \mathbb{X}_4 = \frac{\partial}{\partial z}.$$

Proof: Let $\mathbb{X}$ be a Killing vector field of H_3. We put $\mathbb{X} = X_1e_1 + X_2e_2 + X_3e_3$, where X_i for $i = 1, 2, 3$ are real-valued C^∞ functions on H_3.

$$\frac{\partial X_1}{\partial x} + \frac{y}{2}X_2 + \frac{xy}{4}X_3 = 0, \tag{1}$$

$$\frac{\partial X_2}{\partial y} + \frac{x}{2}X_1 - \frac{xy}{4}X_3 = 0, \tag{2}$$

$$\frac{\partial X_3}{\partial z} = 0, \tag{3}$$

$$\frac{\partial X_2}{\partial x} + \frac{\partial X_1}{\partial y} - 2\left(\frac{y}{4}X_1 + \frac{x}{4}X_2 + \frac{x^2 - y^2}{8}X_3\right) = 0, \tag{4}$$

$$\frac{\partial X_3}{\partial y} + \frac{\partial X_2}{\partial z} - 2\left(\frac{1}{2}X_1 - \frac{y}{4}X_3\right) = 0, \tag{5}$$

$$\frac{\partial X_3}{\partial x} + \frac{\partial X_1}{\partial z} - 2\left(-\frac{1}{2}X_2 - \frac{x}{4}X_3\right) = 0. \tag{6}$$

Equation (5) derived relatively to z becomes

$$\frac{\partial^2 X_2}{\partial z^2} - \frac{\partial X_1}{\partial z} = 0. \tag{7}$$

Equation (6), when derived relative to z, transforms into

$$\frac{\partial^2 X_1}{\partial z^2} + \frac{\partial X_2}{\partial z} = 0.$$

with Eq. (3), one knows

$$\begin{cases} X_1 = f_1(x,y) + f_2(x,y)\cos z + f_3(x,y)\sin z, \\ X_2 = g_1(x,y) - f_3(x,y)\cos z + f_2(x,y)\sin z, \\ X_3 = h(x,y). \end{cases}$$

Equation (1), first derived relative to *z* and then relative to *y*, provides us with

$$\begin{cases} -\dfrac{\partial^2 f_2}{\partial x \partial y} + \dfrac{1}{2} f_3 + \dfrac{y}{2}\dfrac{\partial f_3}{\partial y} = 0, \\ \dfrac{\partial^2 f_3}{\partial x \partial y} + \dfrac{1}{2} f_2 + \dfrac{y}{2}\dfrac{\partial f_2}{\partial y} = 0. \end{cases}$$

Similarly, equation (2) first derived relative to *z* and then relative to *x* gives

$$\begin{cases} \dfrac{\partial^2 f_3}{\partial x \partial y} - \dfrac{1}{2} f_2 - \dfrac{x}{2}\dfrac{\partial f_2}{\partial x} = 0, \\ \dfrac{\partial^2 f_2}{\partial x \partial y} + \dfrac{1}{2} f_3 + \dfrac{x}{2}\dfrac{\partial f_3}{\partial x} = 0. \end{cases}$$

Equation (1), first derived relative to *z* and then multiplied by *x*, yields

$$\begin{cases} \dfrac{xy}{2} f_3 - x\dfrac{\partial f_2}{\partial x} = 0, \\ \dfrac{xy}{2} f_2 + x\dfrac{\partial f_3}{\partial x} = 0. \end{cases}$$

Differentiating equation (1) first with respect to *z* and then multiplying by *y* gives

$$\begin{cases} -\dfrac{xy}{2} f_2 + y\dfrac{\partial f_3}{\partial y} = 0, \\ \dfrac{xy}{2} f_3 + y\dfrac{\partial f_2}{\partial y} = 0. \end{cases}$$

Based on the preceding analysis, it can be deduced that $f_2 = f_3 = 0$.

Consequently, Equation. (7) transforms into

$$\begin{cases} X_1 = f_1(x,y), \\ X_2 = g_1(x,y), \\ X_3 = h(x,y). \end{cases}$$

Taking into account Equations. (5) and (6), it follows that

$$\begin{cases} X_1 = \dfrac{\partial X_3}{\partial y} + \dfrac{y}{2} X_3, \\ X_2 = -\dfrac{\partial X_3}{\partial x} - \dfrac{x}{2} X_3. \end{cases} \quad (8)$$

Upon considering Equations. (1) and (4) in conjunction, it can be deduced that

$$\frac{\partial^2 X_3}{\partial x \partial y} = 0, \ \frac{\partial^2 X_3}{\partial y^2} = \frac{\partial^2 X_3}{\partial x^2}.$$

which means

$$X_3 = \frac{1}{2}\mathcal{C}_1\left(x^2+y^2\right) + \mathcal{C}_2 x + \mathcal{C}_3 y + \mathcal{C}_4.$$

Taking into consideration Eq. (8), it can be inferred that

$$\begin{cases} X_1 = \dfrac{y}{4}\mathcal{C}_1\left(x^2+y^2\right) + \dfrac{\mathcal{C}_2}{2}xy + \dfrac{\mathcal{C}_3}{2}y^2 + \left(\dfrac{\mathcal{C}_4}{2} + \mathcal{C}_1\right)y + \mathcal{C}_3, \\ X_2 = -\dfrac{x}{4}\mathcal{C}_1\left(x^2+y^2\right) - \dfrac{\mathcal{C}_2}{2}x^2 - \dfrac{\mathcal{C}_3}{2}xy - \left(\dfrac{\mathcal{C}_4}{2} + \mathcal{C}_1\right)x + \mathcal{C}_2, \\ X_3 = \dfrac{1}{2}\mathcal{C}_1\left(x^2+y^2\right) + \mathcal{C}_2 x + \mathcal{C}_3 y + \mathcal{C}_4. \end{cases}$$

By sequentially setting $\mathcal{C}_i = 1,\ i = 1,\ 2,\ 3,\ 4$ and $\mathcal{C}_j = 0$ for all $i \neq j,$ we can obtain the Killing vector field in H_3.

Killing Magnetic Curves in H_3

The magnetic curve induced by the i^{th} Killing vector field, which is governed by the Lorentz equation is expressed as follows:

$$\nabla_{\dot\gamma}\dot\gamma = \phi(\dot\gamma) = \mathbb{X}_i \times \dot\gamma.$$

In the orthogonal basis, $\{e_1, e_2, e_3\}$, the velocity vector $\gamma^{\cdot}$ $\dot\gamma$ın be expressed as $\dot\gamma = \dot\gamma^1 e_1 + \dot\gamma^2 e_2 + \dot\gamma^3 e_3$ (the 'dot' indicates a derivative with respect to time). Then we obtain the equation:

$$\nabla_{\dot\gamma}\dot\gamma = \partial_t \dot\gamma^j e_j + \dot\gamma^i \dot\gamma^j \nabla_{e_i} e_j.$$

On the right-hand side of the equation, the vector product is computed utilizing the orthogonal basis within the tangent space of the underlying manifold. By defining $F_{(i)} \equiv \mathbb{X}_i \times \dot\gamma,$ we derive the following expressions:

$$F_{(1)} = \left(-x\dot\gamma^3 - \dot\gamma^2\left(x^2+y^2\right)/2\right)e_1 + \left(\dot\gamma^1\left(x^2+y^2\right)/2 - y\dot\gamma^3\right)e_2 + \left(y\dot\gamma^2 + x\dot\gamma^1\right)e_3,$$

$$\begin{aligned} F_{(2)} &= \left(-\dot\gamma^3 - x\dot\gamma^2\right)e_1 + \left(x\dot\gamma^1\right)e_2 + \left(\dot\gamma^1\right)e_3, \\ F_{(3)} &= \left(-y\dot\gamma^2\right)e_1 + \left(y\dot\gamma^1 - \dot\gamma^3\right)e_2 + \left(\dot\gamma^2\right)e_3, \\ F_{(4)} &= \left(\dot\gamma^2\right)e_1 - \left(\dot\gamma^1\right)e_2. \end{aligned}$$

The relationship between the components of $\dot\gamma$ in the orthonormal basis $(\dot\gamma^i)$ and the coordinate basis $(\dot x^i)$ is straightforwardly expressed as: $\dot\gamma^1 = \dot x,\ \dot\gamma^2 = \dot y,\ \dot\gamma^3 = \dot z + \frac{y}{2}\dot x - \frac{x}{2}\dot y$. By leveraging this relationship, we can subsequently deduce the subsequent magnetic curves as follows:

χ_1−magnetic curves

$$\begin{cases} \ddot x + \dot y\left(\dot z + \dfrac{y}{2}\dot x - \dfrac{x}{2}\dot y\right) = -x\left(\dot z + \dfrac{y}{2}\dot x - \dfrac{x}{2}\dot y\right) - \dfrac{x^2+y^2}{2}\dot y \\ \ddot y - \dot x\left(\dot z + \dfrac{y}{2}\dot x - \dfrac{x}{2}\dot y\right) = -y\left(\dot z + \dfrac{y}{2}\dot x - \dfrac{x}{2}\dot y\right) + \dfrac{x^2+y^2}{2}\dot x \\ \ddot z + \dfrac{y}{2}\ddot x - \dfrac{x}{2}\ddot y = y\dot y + x\dot x \end{cases} \quad (9)$$

χ_2 −magnetic curves

$$\begin{cases} \ddot x + \dot y\left(\dot z + \dfrac{y}{2}\dot x - \dfrac{x}{2}\dot y\right) = -\left(\dot z + \dfrac{y}{2}\dot x - \dfrac{x}{2}\dot y\right) - x\dot y \\ \ddot y - \dot x\left(\dot z + \dfrac{y}{2}\dot x - \dfrac{x}{2}\dot y\right) = x\dot x \\ \ddot z + \dfrac{y}{2}\ddot x - \dfrac{x}{2}\ddot y = \dot x \end{cases} \quad (10)$$

$\chi 3$ −magnetic curves

$$\begin{cases} \ddot{x} + \dot{y}\left(\dot{z} + \frac{y}{2}\dot{x} - \frac{x}{2}\dot{y}\right) = -y\dot{y} \\ \ddot{y} - \dot{x}\left(\dot{z} + \frac{y}{2}\dot{x} - \frac{x}{2}\dot{y}\right) = -\left(\dot{z} + \frac{y}{2}\dot{x} - \frac{x}{2}\dot{y}\right) + y\dot{x} \\ \ddot{z} + \frac{y}{2}\ddot{x} - \frac{x}{2}\ddot{y} = \dot{y} \end{cases} \quad (11)$$

$\chi 4$ magnetic curves

$$\begin{cases} \ddot{x} + \dot{y}\left(\dot{z} + \frac{y}{2}\dot{x} - \frac{x}{2}\dot{y}\right) = -\dot{y} \\ \ddot{y} - \dot{x}\left(\dot{z} + \frac{y}{2}\dot{x} - \frac{x}{2}\dot{y}\right) = \dot{x} \\ \ddot{z} + \frac{y}{2}\ddot{x} - \frac{x}{2}\ddot{y} = 0 \end{cases} \quad (12)$$

Since analytical solutions (excluding the fourth Killing vector) are unattainable and there is a scarcity of small parameters, we contemplate employing the perturbation method for solving the problem. Consequently, we introduce constants B_i (i = 1, 2, 3) to facilitate the application of the perturbation method. Taking Equation. (9) as an illustrative, we compare the three perturbation methods and select the most efficacious one. This selected method is then applied to Eq. (10) and Eq. (11), as outline in detailed below. Furthermore, we will present the comprehensive equations, up to either first or second order, in term of B_i.

Magnetic Trajectory by the First Killing Vector Field
Straightforward Perturbation Method

After weighting constants B1, Equation. (9) can be expressed as,

$$\begin{cases} \ddot{x} + \dot{y}\left(\dot{z} + \frac{y}{2}\dot{x} - \frac{x}{2}\dot{y}\right) = B_1\left(-x\left(\dot{z} + \frac{y}{2}\dot{x} - \frac{x}{2}\dot{y}\right) - \frac{x^2+y^2}{2}\dot{y}\right), \\ \ddot{y} - \dot{x}\left(\dot{z} + \frac{y}{2}\dot{x} - \frac{x}{2}\dot{y}\right) = B_1\left(-y\left(\dot{z} + \frac{y}{2}\dot{x} - \frac{x}{2}\dot{y}\right) + \frac{x^2+y^2}{2}\dot{x}\right), \\ \ddot{z} + \frac{y}{2}\ddot{x} - \frac{x}{2}\ddot{y} = B_1\left(y\dot{y} + x\dot{x}\right). \end{cases}$$

Matching the coefficients of term with identical powers of B_1^0, we can obtain x0, y0, z0 in the equations: $x_0,\ y_0,\ z_0$

$$x_0 = \frac{C_1}{|C_1|}A_1\sin(C_1 t) + A_2\cos(C_1 t),$$
$$y_0 = A_2\sin(C_1 t) - \frac{C_1}{|C_1|}A_1\cos(C_1 t),$$
$$z_0 = C_1\left(1 + \frac{A_1^2 + A_2^2}{2}\right)t.$$

where C_1, A_1, A_2 are constant.

For the first order B_1^1, we have

$$\ddot{x}_1 + \dot{y}_1\left(\dot{z}_0 + \frac{1}{2}y_0\dot{x}_0 - \frac{1}{2}x_0\dot{y}_0\right) +$$
$$\dot{y}_0\left(\dot{z}_1 + \frac{1}{2}y_0\dot{x}_1 + \frac{1}{2}y_1\dot{x}_0 - \frac{1}{2}x_0\dot{y}_1 - \frac{1}{2}x_1\dot{y}_0\right)$$
$$= -x_0\left(\dot{z}_0 + \frac{1}{2}y_0\dot{x}_0 - \frac{1}{2}x_0\dot{y}_0\right) - \frac{1}{2}\dot{y}_0\left(x_0^2 + y_0^2\right),$$

$$\ddot{y}_1 - \dot{x}_1\left(\dot{z}_0 + \frac{1}{2}y_0\dot{x}_0 - \frac{1}{2}x_0\dot{y}_0\right) -$$
$$\dot{x}_0\left(\dot{z}_1 + \frac{1}{2}y_0\dot{x}_1 + \frac{1}{2}y_1\dot{x}_0 - \frac{1}{2}x_0\dot{y}_1 - \frac{1}{2}x_1\dot{y}_0\right)$$
$$= -y_0\left(\dot{z}_0 + \frac{1}{2}y_0\dot{x}_0 - \frac{1}{2}x_0\dot{y}_0\right) + \frac{1}{2}\dot{x}_0\left(x_0^2 + y_0^2\right),$$

$$\ddot{z}_1 + \frac{1}{2}y_0\ddot{x}_1 + \frac{1}{2}y_1\ddot{x}_0 - \frac{1}{2}x_0\ddot{y}_1 - \frac{1}{2}x_1\ddot{y}_0 = y_0\dot{y}_0 + x_0\dot{x}_0.$$

Upon integrating the final equation, we arrive at:

$$\dot{z}_1 + \frac{1}{2}y_0\dot{x}_1 + \frac{1}{2}y_1\dot{x}_0 - \frac{1}{2}x_0\dot{y}_1 - \frac{1}{2}x_1\dot{y}_0 = C_2. \quad (13)$$

where C_2 represents a constant arising from the integration process. By substituting the expression from Eq. (13) into the aforementioned equations, we obtain:

$$x_1 = \frac{C_1}{|C_1|}A_3\sin(C_1 t) + A_4\cos(C_1 t) - A_2 N_1 t\sin(C_1 t) + \frac{C_1}{|C_1|}A_1 N_1 t\cos(C_1 t),$$

$$y_1 = A_4\sin(C_1 t) - \frac{C_1}{|C_1|}A_3\cos(C_1 t) + \frac{C_1}{|C_1|}A_1 N_1 t\sin(C_1 t) + A_2 N_1 t\cos(C_1 t),$$

$$\left(C_2 + A_1A_3C_1 + A_2A_4C_1 + \frac{A_1^2 + A_2^2}{2}N_1\right)t.$$

where A3, A4 are constant, and N_1 is defined as follows:

$$N_1 = C_2 + 1 + \frac{A_1^2 + A_2^2}{2}.$$

For $x = x_0 + B_1x_1,\ y = y_0 + B_1y_1,\ z = z_0 + B_1z_1.$ Refer to

Figure (1) for a detailed comparison of the first-order result versus the numerical solution.

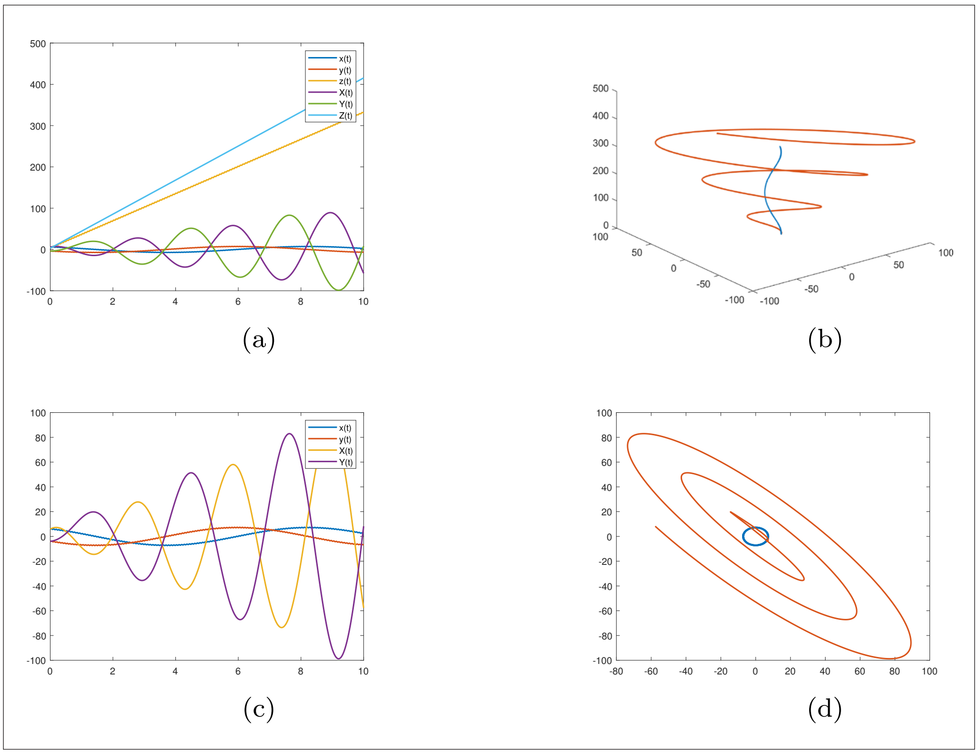

Figure 1: A comparative analysis is conducted between the first-order approximation, visualized through the uppercase plots in Figure (a) and the blue plot in Figure (b), and the numerical solution, represented by the lowercase plots in Figure (a) and the blue plot in Figure (b). To facilitate a more refined observation, Figures (c) and (d) are dedicated solely to the variables ”x, X, y, Y”.

By equating the terms that possess identical powers of B_1^2, we can obtain:

$$
\begin{aligned}
&\ddot{x}_2+\dot{y}_2\left(\dot{z}_0+\frac{1}{2}y_0\dot{x}_0-\frac{1}{2}x_0\dot{y}_0\right)\\
&+\dot{y}_1\left(\dot{z}_1+\frac{1}{2}y_0\dot{x}_1+\frac{1}{2}y_1\dot{x}_0-\frac{1}{2}x_0\dot{y}_1-\frac{1}{2}x_1\dot{y}_0\right)\\
&+\dot{y}_0\left(\dot{z}_2+\frac{1}{2}y_0\dot{x}_2+\frac{1}{2}y_1\dot{x}_1+\frac{1}{2}y_2\dot{x}_0-\frac{1}{2}x_0\dot{y}_2-\frac{1}{2}x_1\dot{y}_1-\frac{1}{2}x_2\dot{y}_0\right)\\
&=-x_1\left(\dot{z}_0+\frac{1}{2}y_0\dot{x}_0-\frac{1}{2}x_0\dot{y}_0\right)\\
&-x_0\left(\dot{z}_1+\frac{1}{2}y_0\dot{x}_1+\frac{1}{2}y_1\dot{x}_0-\frac{1}{2}x_0\dot{y}_1-\frac{1}{2}x_1\dot{y}_0\right)\\
&-\frac{1}{2}\dot{y}_0\left(2x_0x_1+2y_0y_1\right)-\frac{1}{2}\dot{y}_1\left(x_0^2+y_0^2\right),\\
&\ddot{y}_2-\dot{x}_2\left(\dot{z}_0+\frac{1}{2}y_0\dot{x}_0-\frac{1}{2}x_0\dot{y}_0\right)\\
&-\dot{x}_1\left(\dot{z}_1+\frac{1}{2}y_0\dot{x}_1+\frac{1}{2}y_1\dot{x}_0-\frac{1}{2}x_0\dot{y}_1-\frac{1}{2}x_1\dot{y}_0\right)\\
&-\dot{x}_0\left(\dot{z}_2+\frac{1}{2}y_0\dot{x}_2+\frac{1}{2}y_1\dot{x}_1+\frac{1}{2}y_2\dot{x}_0-\frac{1}{2}x_0\dot{y}_2-\frac{1}{2}x_1\dot{y}_1-\frac{1}{2}x_2\dot{y}_0\right)\\
&=-y_1\left(\dot{z}_0+\frac{1}{2}y_0\dot{x}_0-\frac{1}{2}x_0\dot{y}_0\right)\\
&-y_0\left(\dot{z}_1+\frac{1}{2}y_0\dot{x}_1+\frac{1}{2}y_1\dot{x}_0-\frac{1}{2}x_0\dot{y}_1-\frac{1}{2}x_1\dot{y}_0\right)\\
&+\frac{1}{2}\dot{x}_0\left(2x_0x_1+2y_0y_1\right)+\frac{1}{2}\dot{x}_1\left(x_0^2+y_0^2\right),\\
&\ddot{z}_2+\frac{1}{2}y_0\ddot{x}_2+\frac{1}{2}y_1\ddot{x}_1+\frac{1}{2}y_2\ddot{x}_0-\frac{1}{2}x_0\ddot{y}_2-\frac{1}{2}x_1\ddot{y}_1-\frac{1}{2}x_2\ddot{y}_0\\
&=y_0\dot{y}_1+y_1\dot{y}_0+x_0\dot{x}_1+x_1\dot{x}_0.
\end{aligned}
\tag{14}
$$

By solving the integral of the ultimate equation, we derive:

$$\dot{z}_2 + \frac{1}{2}y_0\dot{x}_2 + \frac{1}{2}y_1\dot{x}_1 + \frac{1}{2}y_2\dot{x}_0 - \frac{1}{2}x_0\dot{y}_2 - \frac{1}{2}x_1\dot{y}_1 - \frac{1}{2}x_2\dot{y}_0 = C_3.$$

where C_3 is constant. By using this expression in Eq. (14), we obtain:

$$x_2 = \frac{C_1}{|C_1|}A_5 \sin(C_1 t) + A_6 \cos(C_1 t) + N_3 t \sin(C_1 t) + N_4 t \cos(C_1 t),$$

$$y_2 = A_6 \sin(C_1 t) - \frac{C_1}{|C_1|}A_5 \cos(C_1 t) + \left(N_4 - \frac{A_1 N_1^2}{|C_1|}\right) t \sin(C_1 t) - \left(N_3 + \frac{A_2 N_1^2}{C_1}\right) t \cos(C_1 t),$$

$$\begin{aligned} z_2 =& C_4 + \frac{A_1^2 - A_2^2}{8C_1^2}N_1^2 \sin(2C_1 t) + \frac{A_1 A_2}{4C_1|C_1|}N_1^2 \cos(2C_1 t) + C_3 t + \frac{3}{2}N_1 N_2 t \\ &+ \frac{A_1^2 + A_2^2}{2}\left(C_3 + N_2 + \frac{2C_2 - 2N_1 - N_1^2}{2C_1}\right) t + C_1\left(A_1 A_5 + A_2 A_6 + \frac{A_3^2 + A_4^2}{2}\right) t. \end{aligned}$$

where C_3, C_4, A_5, A_6 are constant, and N_2, N_3, N_4 are defined as follows

$$\begin{aligned} N_2 &= A_1 A_3 + A_2 A_4, \\ N_3 &= \frac{1}{C_1}\left[(A_2 - A_4 C_1) N_1 - C_2 A_2 - C_1 C_3 A_2 - C_1 A_2 N_2\right], \\ N_4 &= -\frac{C_1}{|C_1|}\left[\left(\frac{A_1}{C_1} - A_3\right) N_1 - C_3 A_1 - A_1 N_2 - \frac{C_2 A_1}{C_1}\right]. \end{aligned}$$

For $x = x_0 + B_1 x_1 + B_1^2 x_2$, $y = y_0 + B_1 y_1 + B_1^2 y_2$, $z = z_0 + B_1 z_1 + B_1^2 z_2$. Consult Figure 2 for a detailed comparative assessment of the second-order approximation versus the numerical solution.

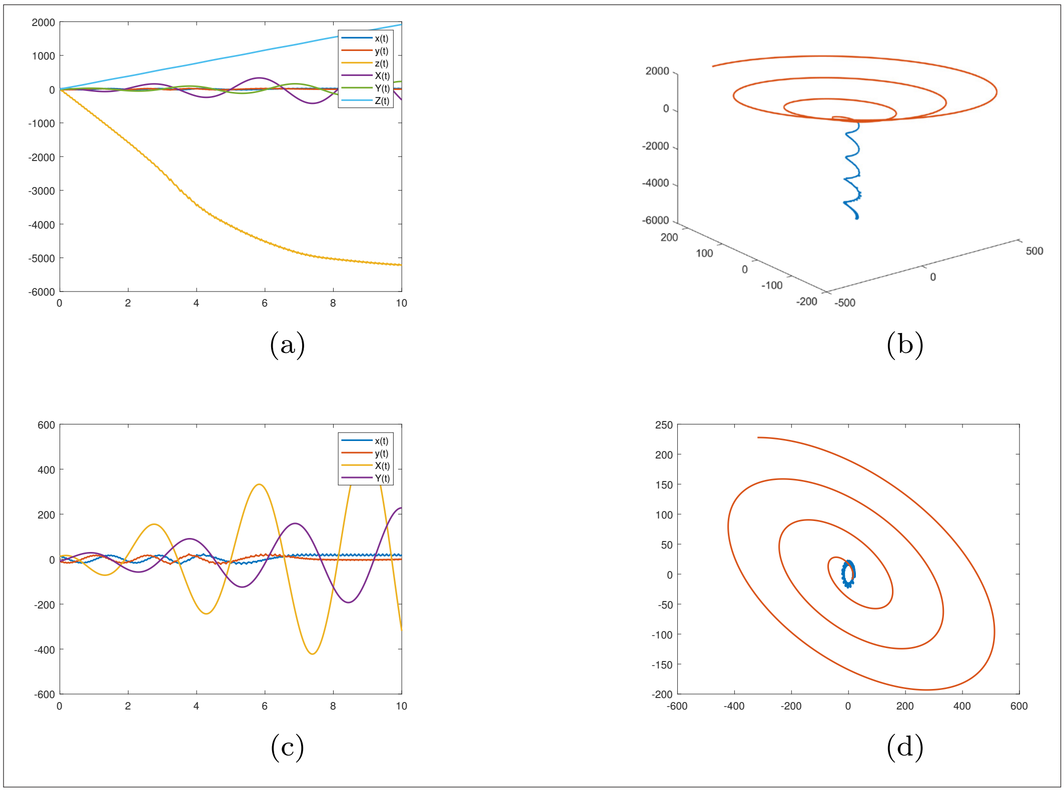

Figure 2: In this analysis, we undertake a comparative examination of the second-order solution, illustrated by the uppercase plots in Figure (a) and the blue plot in Figure (b), against the numerical solution, represented by the lowercase plots in Figure (a) and the corresponding blue plot in Figure (b). To facilitate a clearer understanding, Figures (c) and (d) are presented, which specifically concentrate on the variables "x, X, y, Y." Our findings indicate a notable augmentation in the significance of the secular term as time progresses.

The expressions sin $(C_1 t)$ and cos $(C_1 t)$, represent periodic functions characterized by constant amplitudes. Conversely, the terms t sin $(C_1 t)$ and t cos $(C_1 t)$ exhibit periodicity but with amplitudes that grow linearly with time t. Consequently, it is imperative to implement certain measures to prevent the emergence of secular terms in the resultant solutions.

Lindstedt – Poincare´ Method

To get rid of the secular term, we turn to the Lindstedt – Poincare´ method, referenced in [20]. Since z (t) may not naturally exhibit periodic behavior, we apply both the Lindstedt – Poincare´ method and a direct perturbation method to tackle the differential equation system.

Through the process of integrating the ultimate equation presented in (14), we have:

$$\dot{z} + \frac{y}{2}\dot{x} - \frac{x}{2}\dot{y} - \frac{x^2+y^2}{2} = M,$$

where M is a new constant of integration. We substitute it into the first and second equation in (14), resulting in:

$$\begin{cases} \ddot{x} + M\dot{y} = -Mx - \frac{x^2+y^2}{2}\left(2\dot{y}+x\right), \\ \ddot{y} - M\dot{x} = -My + \frac{x^2+y^2}{2}\left(2\dot{x}-y\right). \end{cases}$$

Subsequently, we set $\tau = \omega t$ and introduce an additional term, B_1:

$$\begin{cases} \omega^2\ddot{x} + \omega M\dot{y} = B_1\left[-Mx - \left(2\omega\dot{y}+x\right)\left(x^2+y^2\right)/2\right], \\ \omega^2\ddot{y} - \omega M\dot{x} = B_1\left[-My + \left(2\omega\dot{x}-y\right)\left(x^2+y^2\right)/2\right]. \end{cases}$$

Define $x = x_0 + B_1 x_1,\ y = y_0 + B_1 y_1,\ z = z_0 + B_1 z_1,$

$$\omega = \omega_0 + B_1\omega_1.$$

Then we equate the terms with corresponding powers of B_1^0:

$$\omega_0^2\ddot{x}_0 + M\omega_0\dot{y}_0 = 0,$$

$$\omega_0^2\ddot{y}_0 - M\omega_0\dot{x}_0 = 0.$$

At this juncture, we recognize that the initial term of the frequency series must coincide with the natural frequency, $\omega_0 = M$. Consequently, we know:

$$x_0 = A_1\sin\tau + A_2\cos\tau,$$

$$y_0 = A_2\sin\tau - A_1\cos\tau.$$

By equating the terms that have the same powers of B_1^1:

$$\omega_0^2\ddot{x}_1 + 2\omega_0\omega_1\ddot{x}_0 + \omega_0 M\dot{y}_1 + \omega_1 M\dot{y}_0 = -Mx_0 - \frac{x_0^2+y_0^2}{2}\left(2\omega_0\dot{y}_0 + x_0\right),$$

$$\omega_0^2\ddot{y}_1 + 2\omega_0\omega_1\ddot{y}_0 - \omega_0 M\dot{x}_1 - \omega_1 M\dot{x}_0 = -My_0 + \frac{x_0^2+y_0^2}{2}\left(2\omega_0\dot{x}_0 - y_0\right).$$

By substituting x_0 and y_0 into the previously derived equations,

$$M^2\left(\ddot{x}_1 + \dot{y}_1\right) = \left[M\omega_1 - M - \frac{A_1^2+A_2^2}{2}\left(2M+1\right)\right]\left(A_1\sin\tau + A_2\cos\tau\right),$$

$$M^2\left(\ddot{y}_1 - \dot{x}_1\right) = \left[M\omega_1 - M - \frac{A_1^2+A_2^2}{2}\left(2M+1\right)\right]\left(A_2\sin\tau - A_1\cos\tau\right).$$

The inclusion of sin τ and cos τ terms will result in secular contributions within the solutions for x_1 and y_1. To eliminate the emergence of these secular terms, we determine ω_1 in such a way that the coefficients of sin τ and cos τ rendered zero

$$\omega_1 = \frac{M + \frac{1}{2}\left(A_1^2+A_2^2\right)\left(2M+1\right)}{M}.$$

The remaining set of equations will then be

$$M^2\left(\ddot{x}_1 + \dot{y}_1\right) = 0,$$

$$M^2\left(\ddot{y}_1 - \dot{x}_1\right) = 0.$$

whose solutions entail

$$x_1 = A_3\sin t + A_4\cos t,$$

$$y_1 = A_4\sin t - A_3\cos t.$$

For the expressions $x = x_0 + B_1 x_1,\ y = y_0 + B_1 y_1,$ $z = z_0 + B_1 z_1$, we can obtain the following numerical values:

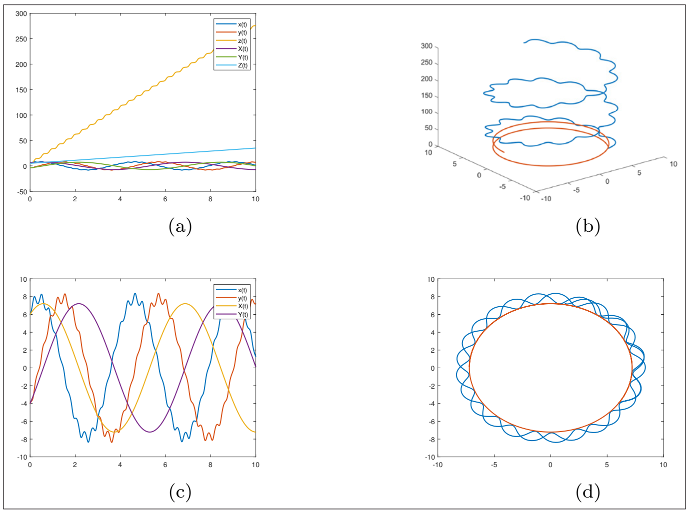

Figure 3: In this comparison, we showcase the first-order solution using uppercase letters in Figure (a) and the corresponding blue plot in Figure (b). Similarly, the numerical solution is represented by lowercase letters in Figure (a) and the same blue plot in Figure (b). For better visualization, Figures (c) and (d) are provided,

which specifically concentrate on the variables 'x, X, y, Y'.

Our analysis reveals that the solution obtained through the Lindstedt – Poincare´ method exhibits a higher degree of proximity to the numerical solution than those presented in section 4.1.1.

Homotopy Perturbation Method

Due to the stringent requirement of the existence of a small parameter, traditional perturbation techniques are not universally applicable. To overcome the limita- tion posed by the" small parameter," Liu introduced the artificial parameter method, while Liao proposed the homotopy analysis method. Furthermore, He has expertly utilized these methods to develop a novel perturbation approach known as the homotopy perturbation method [21-23].

If the set of differential equation is accompanied by initial conditions

$$x(0) = P_1,\ \dot{x}(0) = P_2,\ y(0) = P_2,\ \dot{y}(0) = P_1,\ z(0) = P_4,\ \dot{z}(0) = P_3, \qquad (15)$$

where P_1, P_2, P_3, P_4 are constant.

We postulate the initial approximate form of Eq. (15) as

$$\begin{cases} x_0(t) = P_1\cos(t) + P_2\sin(t), \\ y_0(t) = P_2\cos(t) + P_1\sin(t), \\ z_0(t) = P_4 t + P_3. \end{cases}$$

And we can establish the following homotopy

$$\begin{cases} \ddot{X} - \ddot{x}_0 = B_1\left[-\ddot{x}_0 - \left(X + \dot{Y}\right)\left(\dot{Z} + \frac{Y}{2}\dot{X} - \frac{X}{2}\dot{Y}\right) - \frac{\dot{Y}}{2}\left(X^2 + Y^2\right)\right], \\ \ddot{Y} - \ddot{y}_0 = B_1\left[-\ddot{y}_0 + \left(\dot{X} - Y\right)\left(\dot{Z} + \frac{Y}{2}\dot{X} - \frac{X}{2}\dot{Y}\right) + \frac{\dot{X}}{2}\left(X^2 + Y^2\right)\right], \\ \ddot{Z} - \ddot{z}_0 = B_1\left[-\ddot{z}_0 + \frac{1}{2}X\ddot{Y} - \frac{1}{2}Y\ddot{X} + X\dot{X} + Y\dot{Y}\right]. \end{cases}$$

Matching the coefficients for terms involving identical powers of B_1^0 ,

$$\begin{cases} X_0 = P_1\cos(t) + P_2\sin(t), \\ Y_0 = P_2\cos(t) + P_1\sin(t), \\ Z_0 = P_4 t + P_3. \end{cases} \qquad (16)$$

Equating the coefficients of terms with identical powers of B_1^1,

$$\ddot{X}_1 = -\ddot{x}_0 - \left(X_0 + \dot{Y}_0\right)\left(\dot{Z}_0 + \frac{Y_0}{2}\dot{X}_0 - \frac{X_0}{2}\dot{Y}_0\right) - \frac{\dot{Y}_0}{2}\left(X_0^2 + Y_0^2\right),$$

$$\ddot{Y}_1 = -\ddot{y}_0 + \left(\dot{X}_0 - Y_0\right)\left(\dot{Z}_0 + \frac{Y_0}{2}\dot{X}_0 - \frac{X_0}{2}\dot{Y}_0\right) + \frac{\dot{X}_0}{2}\left(X_0^2 + Y_0^2\right),$$

$$\ddot{Z}_1 = -\ddot{z}_0 + \frac{1}{2}X_0\ddot{Y}_0 - \frac{1}{2}Y_0\ddot{X}_0 + X_0\dot{X}_0 + Y_0\dot{Y}_0.$$

Upon incorporation of Eq. (16) into the equation, we attain:

$$\begin{cases} X_1 = -Q_2\sin t + (Q_3 + 2P_1Q_1)\cos t + \frac{2}{9}P_1P_2^2\cos^3 t - \frac{2}{9}P_1^2P_2\sin^3 t, \\ Y_1 = -Q_2\cos t + (Q_3 + 2P_1Q_1)\sin t - \frac{2}{9}P_1^2P_2\cos^3 t + \frac{2}{9}P_1P_2^2\sin^3 t, \\ Z_1 = -\frac{1}{4}P_1P_2\cos(2t). \end{cases} \qquad (17)$$

The values of $Q1, Q2, Q3$ are as detailed below:

$$Q_1 = P_4 + \frac{1}{2}\left(P_1^2 + P_2^2\right), Q_2 = P_2 + \frac{1}{2}P_2^3 - \frac{1}{6}P_1^2P_2,$$

$$Q_3 = -P_1 + \frac{1}{2}P_1^3 - \frac{1}{6}P_1P_2^2.$$

Given the expressions $X = X_0 + B_1X_1$, $Y = Y_0 + B_1Y_1$, $Z = Z_0 + B_1Z_1$, we can derive the subsequent numerical values,

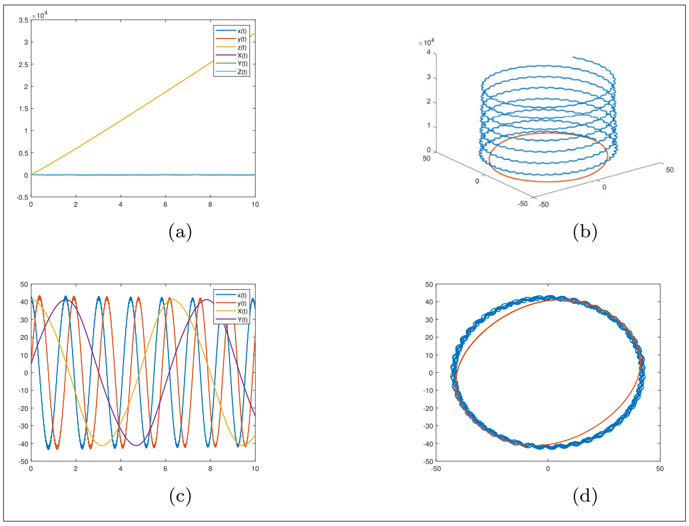

Figure 4: We pit the first-order solution, vividly captured by the uppercase plots in Figure (a) and the striking blue plot in Figure (b), against the numerical solution, portrayed by the lowercase plots in Figure (a) and the same captivating blue plot. To enhance clarity, Figures (c) and (d) zoom in on the crucial variables 'x, X, y, Y'.

Equating coefficients for terms with B_1^2 raised to the same power

$$\begin{aligned} \ddot{X}_2 = &-\left(X_0 + \dot{Y}_0\right)\left(\dot{Z}_1 + \frac{1}{2}Y_1\dot{X}_0 + \frac{1}{2}Y_0\dot{X}_1 - \frac{1}{2}X_0\dot{Y}_1 - \frac{1}{2}X_1\dot{Y}_0\right) \\ &-\left(X_1 + \dot{Y}_1\right)\left(\dot{Z}_0 + \frac{Y_0}{2}\dot{X}_0 - \frac{X_0}{2}\dot{Y}_0\right) \\ &-\frac{1}{2}\dot{Y}_0\left(2X_0X_1 + 2Y_0Y_1\right) - \frac{1}{2}\dot{Y}_1\left(X_0^2 + Y_0^2\right), \end{aligned}$$

$$\begin{aligned} \ddot{Y}_2 = &\left(\dot{X}_0 - Y_0\right)\left(\dot{Z}_1 + \frac{1}{2}Y_1\dot{X}_0 + \frac{1}{2}Y_0\dot{X}_1 - \frac{1}{2}X_0\dot{Y}_1 - \frac{1}{2}X_1\dot{Y}_0\right) \\ &+\left(\dot{X}_1 - Y_1\right)\left(\dot{Z}_0 + \frac{Y_0}{2}\dot{X}_0 - \frac{X_0}{2}\dot{Y}_0\right) \\ &+\frac{1}{2}\dot{X}_0\left(2X_0X_1 + 2Y_0Y_1\right) + \frac{1}{2}\dot{X}_1\left(X_0^2 + Y_0^2\right), \end{aligned}$$

$$\ddot{Z}_2 = \frac{1}{2}X_0\ddot{Y}_1 + \frac{1}{2}X_1\ddot{Y}_0 - \frac{1}{2}Y_0\ddot{X}_1 - \frac{1}{2}Y_1\ddot{X}_0 + \dot{Y}_0Y_1 + \dot{Y}_1Y_0 + \dot{X}_1X_0 + \dot{X}_0X_1.$$

Through the substituting the Eqs. (16) and (17), we have

$$= \left(Q_4 - \frac{1}{6}P_1^2Q_2 + \frac{29}{135}P_1^2P_2^3\right)\sin t - \left(Q_5 + \frac{43}{135}P_1^3P_2^2 - \frac{1}{27}P_1P_2^4\right)\cos t$$

$$+\frac{1}{3}\left(Q_6 + \frac{2}{3}P_1^2Q_2 + \frac{7}{135}P_1^2P_2^3\right)\sin^3 t - \frac{1}{3}$$

$$\left(Q_7 - \frac{2}{3}P_1^2Q_3 + \frac{1}{27}P_1P_2^4 + \frac{29}{135}P_1^3P_2^2\right)\cos^3 t$$

$$+\left(-\frac{4}{75}P_1^2P_2^3\right)\sin^5 t-\left(-\frac{4}{225}P_1^3P_2^2\right)\cos^5 t,$$

$$Y_2=-\left(Q_5+\frac{73}{135}P_1^3P_2^2+\frac{5}{27}P_1P_2^4\right)\sin t+\left(Q_4+\frac{1}{2}P_1^2Q_2+\frac{38}{45}P_1^2P_2^3\right)\cos t$$
$$+\frac{1}{3}\left(-Q_7+\frac{5}{27}P_1P_2^4+\frac{2}{3}P_2^2Q_3+\frac{1}{135}P_1^3P_2^2\right)\sin^3 t-\frac{1}{3}\left(-Q_6+\frac{26}{45}P_1^2P_2^3\right)\cos^3 t$$
$$+\left(\frac{4}{225}P_1^3P_2^2\right)\sin^5 t-\left(\frac{4}{75}P_1^2P_2^3\right)\cos^5 t,$$

$$Z_2=\frac{1}{2}\left[P_1Q_2-P_2\left(Q_3+2P_1Q_1\right)-\frac{2}{9}P_1P_2^3\right]\cos\left(2t\right)+\frac{1}{3}P_1^2P_2^2t+\frac{1}{36}P_1^2P_2^2\sin\left(4t\right).$$

The expressions for $Q4$, Q5, Q6, Q7 are given as follows,

$$Q_4=\frac{3}{2}P_2^2Q_2+\frac{2}{3}P_1^2P_2-\frac{1}{9}P_1^4P_2+\frac{20}{27}P_1^2P_2Q_1+\frac{1}{3}P_1P_2Q_3,$$
$$Q_5=\frac{5}{3}P_1P_2Q_2-\frac{1}{27}P_1P_2^2Q_1+\frac{1}{6}P_2^2Q_3+P_1^3Q_1+\frac{1}{2}P_1^2Q_3-2Q_1Q_3-4P_1Q_1^2,$$
$$Q_6=-\frac{2}{3}P_1^2P_2-\frac{80}{27}P_1^2P_2Q_1-\frac{4}{3}P_1P_2Q_3+\frac{1}{9}P_1^4P_2,$$
$$Q_7=-\frac{32}{27}P_1P_2^2Q_1+\frac{4}{3}P_1P_2Q_2.$$

For the equations

$X=X_0+B_1X_1+B_1^2X_2$, $Y=Y_0+B_1Y_1+B_1^2Y_2$, and $Z=Z_0+B_1Z_1+B_1^2Z_2$, we can obtain the following figures,

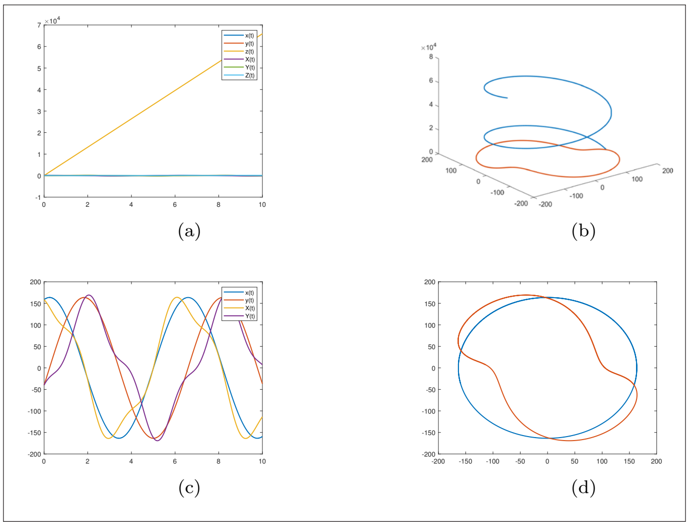

Figure 5: A comparative assessment is conducted between the second-order solution, which is illustrated by the uppercase plots in Figure (a) and the blue plot in Figure (b), and the numerical solution, represented by the lowercase plots in Figure (a) and the corresponding blue plot. To enhance clarity and facilitate analysis, Figures (c) and (d) are provided, focusing solely on the variables x, X, y, and Y.

It is evident that the solution obtained through the homotopy perturbation method is the most proximate numerical solution among the three methodologies, and the second-order solution demonstrates superior performance compared to the first-order solution.

Magnetic Trajectory by the Second Killing Vector Field

If the set of differential equations is equipped with initial conditions

$$x\left(0\right)=Q_1P_5,\ \dot{x}\left(0\right)=P_5,\ y\left(0\right)=Q_1P_6,\ \dot{y}\left(0\right)=P_6,$$

$$z\left(0\right)=-\frac{P_6}{Q_1},\ \dot{z}\left(0\right)=P_6. \quad (18)$$

where $P5$, P6, $Q1$ are constant.

We postulate that the initial approximate pertaining to Eq. (18) possesses the following form:

$$\begin{cases} x_0\left(t\right)=Q_1P_5\cos\left(t\right)+P_5\sin\left(t\right),\\ y_0\left(t\right)=Q_1P_6\cos\left(t\right)+P_6\sin\left(t\right),\\ z_0\left(t\right)=-\dfrac{P_6}{Q_1}\cos\left(t\right)+P_6\sin\left(t\right).\end{cases}$$

We can formulate the subsequent homotopy:

$$\begin{cases}\ddot{X}-\ddot{x}_0=B_2\left[-\ddot{x}_0-\left(1+\dot{Y}\right)\left(\dot{Z}+\dfrac{Y}{2}\dot{X}-\dfrac{X}{2}\dot{Y}\right)-X\dot{Y}\right],\\ \ddot{Y}-\ddot{y}_0=B_2\left[-\ddot{y}_0+\dot{X}\left(\dot{Z}+\dfrac{Y}{2}\dot{X}-\dfrac{X}{2}\dot{Y}\right)+\dot{X}X\right],\\ \ddot{Z}-\ddot{z}_0=B_2\left[-\ddot{z}_0+\dfrac{1}{2}X\ddot{Y}-\dfrac{1}{2}Y\ddot{X}+\dot{X}\right].\end{cases}$$

We equate the terms with identical powers of B_2^0 by matching their coefficients,

$$\begin{cases}X_0=Q_1P_5\cos\left(t\right)+P_5\sin\left(t\right),\\ Y_0=Q_1P_6\cos\left(t\right)+P_6\sin\left(t\right),\\ Z_0=-\frac{P_6}{Q_1}\cos\left(t\right)+P_6\sin\left(t\right).\end{cases} \quad (19)$$

By equating the terms that possess the identical powers of B_2^1,

$$\ddot{X}_1=-\ddot{x}_0-\left(1+\dot{Y}_0\right)\left(\dot{Z}_0+\frac{Y_0}{2}\dot{X}_0-\frac{X_0}{2}\dot{Y}_0\right)-\dot{Y}_0X_0,$$
$$\ddot{Y}_1=-\ddot{y}_0+\dot{X}_0\left(\dot{Z}_0+\frac{Y_0}{2}\dot{X}_0-\frac{X_0}{2}\dot{Y}_0\right)+\dot{X}_0X_0,$$
$$\ddot{Z}_1=-\ddot{z}_0+\frac{1}{2}X_0\ddot{Y}_0-\frac{1}{2}Y_0\ddot{X}_0+\dot{X}_0.$$

Substituting Eq. (19) gives

$$\begin{cases}X_1=-\dfrac{M_{22}}{Q_1}\sin\left(t\right)-M_{22}\cos\left(t\right)+\dfrac{1}{8}M_{21}P_6\left(\dfrac{1}{Q_1}-Q_1\right)\sin\left(2t\right)+\dfrac{M_{21}P_6}{4}\cos\left(2t\right),\\ Y_1=-P_6\sin\left(t\right)-Q_1P_6\cos\left(t\right)-\dfrac{1}{8}M_{22}P_5\left(\dfrac{1}{Q_1}-Q_1\right)\sin\left(2t\right)-\dfrac{M_{22}P_5}{4}\cos\left(2t\right),\\ Z_1=M_{21}\sin\left(t\right)-\dfrac{M_{21}}{Q_1}\cos\left(t\right).\end{cases} \quad (20)$$

The expressions of $M22$, $M22$ are as follows,

$$M_{21}=Q_1P_5-P_6,\ M_{22}=Q_1P_5+P_6.$$

Equating the coefficients of terms with identical powers of B_2^2,

$$\ddot{X}_2=-\left(1+\dot{Y}_0\right)\left(\dot{Z}_1+\frac{1}{2}Y_1\dot{X}_0+\frac{1}{2}Y_0\dot{X}_1-\frac{1}{2}X_0\dot{Y}_1-\frac{1}{2}X_1\dot{Y}_0\right)$$
$$-\dot{Y}_1\left(\dot{Z}_0+\frac{Y_0}{2}\dot{X}_0-\frac{X_0}{2}\dot{Y}_0\right)-\dot{Y}_1X_0-\dot{Y}_0X_1,$$
$$\ddot{Y}_2=\dot{X}_0\left(\dot{Z}_1+\frac{1}{2}Y_1\dot{X}_0+\frac{1}{2}Y_0\dot{X}_1-\frac{1}{2}X_0\dot{Y}_1-\frac{1}{2}X_1\dot{Y}_0\right)$$
$$+\dot{X}_1\left(\dot{Z}_0+\frac{Y_0}{2}\dot{X}_0-\frac{X_0}{2}\dot{Y}_0\right)+\dot{X}_1X_0+\dot{X}_0X_1,$$
$$\ddot{Z}_2=\frac{X_1}{2}\ddot{Y}_0+\frac{X_0}{2}\ddot{Y}_1-\frac{Y_1}{2}\ddot{X}_0-\frac{Y_0}{2}\ddot{X}_1+\dot{X}_1.$$

Upon substitution of Eqs. (19) and (20), we arrive at

$$\begin{aligned}X_2 =& M_{23}\sin(t) + M_{23}Q_1\cos(t) + \frac{1}{8}\left(Q_1 - \frac{1}{Q_1}\right) \\ & M_{24}\sin(2t) - \frac{1}{4}M_{24}\cos(2t) \\ &+ \frac{1}{9}\left(3 - \frac{1}{Q_1^2}\right)M_{25}\sin(3t) + \frac{1}{9}\left(Q_1 - \frac{3}{Q_1}\right)M_{25}\cos(3t) \\ &+ \frac{1}{1024}P_6\left(M_{22}P_5^2 + M_{21}P_6^2\right)\left(Q_1^3 - 6Q_1 + \frac{1}{Q_1}\right)\sin(4t) \\ &+ \frac{1}{256}P_6\left(M_{22}P_5^2 + M_{21}P_6^2\right)\left(1 - Q_1^2\right)\cos(4t), \\ =& -M_{26}\sin(t) - M_{26}Q_1\cos(t) + \frac{1}{8}\left(\frac{1}{Q_1} - Q_1\right) \\ & M_{27}\sin(2t) + \frac{1}{4}M_{27}\cos(2t) \\ &+ \frac{1}{9}\left(3 - \frac{1}{Q_1^2}\right)M_{28}\sin(3t) + \frac{1}{9}\left(Q_1 - \frac{3}{Q_1}\right)M_{28}\cos(3t) \\ &+ \frac{1}{1024}P_5\left(M_{22}P_5^2 + M_{21}P_6^2\right)\left(-Q_1^3 + 6Q_1 - \frac{1}{Q_1}\right)\sin(4t) \\ &+ \frac{1}{256}P_5\left(M_{22}P_5^2 + M_{21}P_6^2\right)\left(Q_1^2 - 1\right)\cos(4t), \\ Z_2 =& \frac{1}{2}\left(3\frac{M_{24}}{P_6} - 5M_{22}\right)\sin(t) + \frac{1}{2Q_1}\left(3\frac{M_{24}}{P_6} - 5M_{22}\right)\cos(t) \\ &+ \frac{1}{8}M_{21}P_6\sin(2t) + \frac{1}{16}M_{21}P_6\left(Q_1 - \frac{1}{Q_1}\right)\cos(2t) \\ &+ \frac{1}{96}\left(M_{22}P_5^2 + M_{21}P_6^2\right)\left(Q_1^2 - 3\right)\sin(3t) \\ &+ \frac{1}{96}\left(M_{22}P_5^2 + M_{21}P_6^2\right)\left(\frac{1}{Q_1} - 3Q_1\right)\cos(3t).\end{aligned}$$

the M_{23}, M_{24}, M_{25}, M_{26}, M_{27}, M_{28} are as follows,

$$\begin{aligned}M_{23} =& \frac{1}{16}M_{21}P_6^2\left(\frac{1}{Q_1} + Q_1\right) + \frac{1}{8}M_{22}^2P_5\left(\frac{1}{Q_1^2} + 1\right) + \\ & \frac{M_{21}}{Q_1} - \frac{3}{32}\left(\frac{1}{Q_1} + Q_1\right)\left(M_{21}P_6^2 + M_{22}P_5^2\right),\end{aligned}$$

$$\begin{aligned}M_{24} &= \frac{1}{16}P_6\left(1 + Q_1^2\right)\left(M_{21}P_6^2 + M_{22}P_5^2\right) + M_{22}P_6, \\ M_{25} &= \frac{1}{32}Q_1\left(-M_{21}P_6^2 + M_{22}P_5^2\right) + \frac{1}{8}M_{22}^2P_5, \\ M_{26} &= \frac{1}{16}M_{21}P_5P_6\left(\frac{1}{Q_1} + Q_1\right) - \frac{1}{8}M_{21}M_{22}P_6\left(\frac{1}{Q_1^2} + 1\right), \\ M_{27} &= \frac{1}{16}P_5\left(1 + Q_1^2\right)\left(M_{21}P_6^2 + M_{22}P_5^2\right) + \frac{M_{22}^2}{Q_1}, \\ M_{28} &= \frac{1}{16}M_{21}P_5P_6Q_1 + \frac{1}{8}M_{21}M_{22}P_6.\end{aligned}$$

Given the expressions $X = X_0 + B_1X_1 + B_1^2X_2$, $Y = Y_0 + B_1Y_1 + B_1^2Y_2$, and $Z = Z_0 + B_1Z_1 + B_1^2Z_2$,

we can derive the subsequent numerical values:

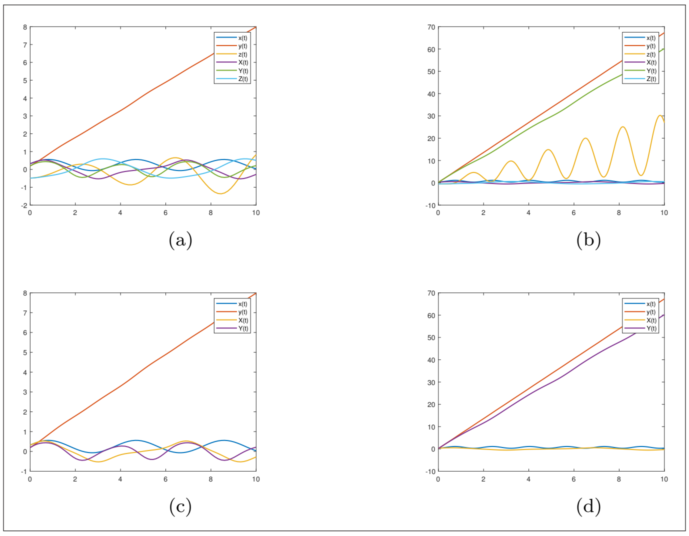

Figure 6: Herein, we undertake a comparative evaluation of the second-order solution, denoted by the uppercase graphical representations in Figure (a), against the numerical solution, represented by the lowercase graphical representations in the same figure. Additionally, given the inherent uncertainty surrounding the term σt(*where* σ is *constant*) in the integration process of the aforementioned solutions, we further present a solution that accounts for this term in Figure (b). For the purpose of enhancing clarity and ease of observation, we have included Figures (c) and (d), which exclusively pertain to the variables ”x, X, y, Y”.

It is readily apparent that the first-order solution exhibits superior performance compared to the second-order solution.

Magnetic Trajectory by the Third Killing Vector Field

If the differential equations have initial conditions

$$x(0) = Q_2P_7,\ \dot{x}(0) = P_7,\ y(0) = Q_2P_8,\ \dot{y}(0) = P_8,$$
$$z(0) = -\frac{P_7}{Q_2},\ \dot{z}(0) = P_7. \qquad (21)$$

where P_7, P_8, Q_2 are constant.

We postulate that the initial approximate of Eq. (21) adopts the form

$$\begin{cases} x_0(t) = Q_2P_7\cos(t) + P_7\sin(t), \\ y_0(t) = Q_2P_8\cos(t) + P_8\sin(t), \\ z_0(t) = -\frac{P_8}{Q_2}\cos(t) + P_8\sin(t). \end{cases}$$

We can establish the following homotopy

$$\begin{cases} \ddot{X} - \ddot{x}_0 = B_3\left[-\ddot{x}_0 - \dot{Y}\left(\dot{Z} + \frac{Y}{2}\dot{X} - \frac{X}{2}\dot{Y}\right) - Y\dot{Y}\right], \\ \ddot{Y} - \ddot{y}_0 = B_3\left[-\ddot{y}_0 + \left(\dot{X} - 1\right)\left(\dot{Z} + \frac{Y}{2}\dot{X} - \frac{X}{2}\dot{Y}\right) + \dot{X}Y\right], \\ \ddot{Z} - \ddot{z}_0 = B_3\left[-\ddot{z}_0 + \frac{1}{2}X\ddot{Y} - \frac{1}{2}Y\ddot{X} + \dot{Y}\right]. \end{cases}$$

Equating coefficients of like terms powers of B_3^0:

$$\begin{cases} X_0 = Q_2P_7\cos(t) + P_7\sin(t), \\ Y_0 = Q_2P_8\cos(t) + P_8\sin(t), \\ Z_0 = -\frac{P_7}{Q_2}\cos(t) + P_7\sin(t). \end{cases} \qquad (22)$$

Matching B_3^1 powers we have:

$$\ddot{X}_1 = -\ddot{x}_0 - \dot{Y}_0\left(\dot{Z}_0 + \frac{Y_0}{2}\dot{X}_0 - \frac{X_0}{2}\dot{Y}_0\right) - \dot{Y}_0 Y_0,$$
$$\ddot{Y}_1 = -\ddot{y}_0 + \left(\dot{X}_0 - 1\right)\left(\dot{Z}_0 + \frac{Y_0}{2}\dot{X}_0 - \frac{X_0}{2}\dot{Y}_0\right) + \dot{X}_0 Y_0,$$
$$\ddot{Z}_1 = -\ddot{z}_0 + \frac{1}{2}X_0\ddot{Y}_0 - \frac{1}{2}Y_0\ddot{X}_0 + \dot{Y}_0.$$

Substituting Eq. (22) yields

$$\begin{cases} X_1 = -P_7\sin(t) - Q_2P_7\cos(t) + \frac{1}{8}M_{32}P_8\left(\frac{1}{Q_2} - Q_2\right)\sin(2t) + \frac{P_8M_{32}}{4}\cos(2t), \\ Y_1 = -\frac{M_{31}}{Q_2}\sin(t) - M_{31}\cos(t) - \frac{1}{8}M_{32}P_7\left(\frac{1}{Q_2} - Q_2\right)\sin(2t) - \frac{P_7M_{32}}{4}\cos(2t), \\ Z_1 = M_{31}\sin(t) - \frac{M_{31}}{Q_2}\cos(t). \end{cases} \quad (23)$$

M_{31}, M_{31} are denoted as,

$$M_{31} = Q_2P_8 - P_7, \ M_{32} = Q_2P_8 + P_7.$$

By aligning the terms with equivalent powers of B_3^2 and equating their coefficients,

$$\ddot{X}_2 = -\dot{Y}_0\left(\dot{Z}_1 + \frac{1}{2}Y_1\dot{X}_0 + \frac{1}{2}Y_0\dot{X}_1 - \frac{1}{2}X_0\dot{Y}_1 - \frac{1}{2}X_1\dot{Y}_0\right)$$
$$-\dot{Y}_1\left(\dot{Z}_0 + \frac{Y_0}{2}\dot{X}_0 - \frac{X_0}{2}\dot{Y}_0\right) - \dot{Y}_1Y_0 - \dot{Y}_0Y_1,$$
$$\ddot{Y}_2 = \left(\dot{X}_0 - 1\right)\left(\dot{Z}_1 + \frac{1}{2}Y_1\dot{X}_0 + \frac{1}{2}Y_0\dot{X}_1 - \frac{1}{2}X_0\dot{Y}_1 - \frac{1}{2}X_1\dot{Y}_0\right)$$
$$+\dot{X}_1\left(\dot{Z}_0 + \frac{Y_0}{2}\dot{X}_0 - \frac{X_0}{2}\dot{Y}_0\right) + \dot{X}_1Y_0 + \dot{X}_0Y_1,$$
$$\ddot{Z}_2 = \frac{X_1}{2}\ddot{Y}_0 + \frac{X_0}{2}\ddot{Y}_1 - \frac{Y_1}{2}\ddot{X}_0 - \frac{Y_0}{2}\ddot{X}_1 + \dot{Y}_1.$$

By incorporating Eqs. (22) and (23) into the pertinent formulations, we derive the following results:

$$X_2 = M_{33}\sin(t) + M_{33}Q_2\cos(t) + \frac{1}{8}\left(Q_2 - \frac{1}{Q_2}\right)M_{34}\sin(2t) - \frac{1}{4}M_{34}\cos(2t)$$
$$+\frac{1}{9}\left(3 - \frac{1}{Q_2^2}\right)M_{35}\sin(3t) + \frac{1}{9}\left(Q_2 - \frac{3}{Q_2}\right)M_{35}\cos(3t)$$
$$+\frac{1}{1024}M_{32}P_8\left(P_7^2 + P_8^2\right)\left(Q_2^3 - 6Q_2 + \frac{1}{Q_2}\right)\sin(4t)$$
$$+\frac{1}{256}M_{32}P_8\left(P_7^2 + P_8^2\right)\left(1 - Q_2^2\right)\cos(4t),$$
$$Y_2 = M_{36}\sin(t) + M_{36}Q_2\cos(t) + \frac{1}{8}\left(\frac{1}{Q_2} - Q_2\right)M_{37}\sin(2t) + \frac{1}{4}M_{37}\cos(2t)$$
$$+\frac{1}{9}\left(3 - \frac{1}{Q_2^2}\right)M_{38}\sin(3t) + \frac{1}{9}\left(Q_2 - \frac{3}{Q_2}\right)M_{38}\cos(3t)$$
$$+\frac{1}{1024}M_{32}P_7\left(P_7^2 + P_8^2\right)\left(-Q_2^3 + 6Q_2 - \frac{1}{Q_2}\right)\sin(4t)$$
$$+\frac{1}{256}M_{32}P_7\left(P_7^2 + P_8^2\right)\left(Q_2^2 - 1\right)\cos(4t),$$
$$Z_2 = -\left(M_{31} + \frac{3}{16}P_7P_8M_{32}\left(1 + Q_2^2\right)\right)\sin(t)$$
$$+\left(\frac{M_{31}}{Q_2} + \frac{3}{16}P_7P_8M_{32}\left(Q_2 + \frac{1}{Q_2}\right)\right)\cos(t)$$
$$-\frac{1}{8}P_7M_{32}\sin(2t) + \frac{1}{16}P_7M_{32}\left(\frac{1}{Q_2} - Q_2\right)\cos(2t)$$
$$+\frac{1}{48}P_7P_8M_{32}\left(3 - Q_2^2\right)\sin(3t) - \frac{1}{48}P_7P_8M_{32}\left(\frac{1}{Q_2} - 3Q_2\right)\cos(3t).$$

The expressions of $M_{33}, M_{34}, M_{35}, M_{36}, M_{37}, M_{38}$ are as follows,

$$M_{33} = -\frac{1}{16}M_{32}P_7P_8\left(\frac{1}{Q_2} + Q_2\right) + \frac{1}{8}M_{31}M_{32}P_7\left(\frac{1}{Q_2^2} + 1\right),$$
$$M_{34} = \frac{1}{16}M_{32}P_8\left(1 + Q_1^2\right)\left(P_7^2 + P_8^2\right) + \frac{M_{31}^2}{Q_2},$$
$$M_{35} = \frac{1}{16}M_{32}P_7P_8Q_2 + \frac{1}{8}M_{31}M_{32}P_7,$$
$$M_{36} = \frac{M_{31}}{Q_2} + \frac{3}{32}M_{32}\left(P_7^2 + P_8^2\right)\left(\frac{1}{Q_2} + Q_2\right) + \frac{1}{16}M_{32}P_7\left(\frac{1}{Q_2} + Q_2\right) + \frac{1}{8}M_{32}^2P_8\left(\frac{1}{Q_1^2} + 1\right),$$
$$M_{37} = \frac{1}{16}M_{32}P_7\left(1 + Q_2^2\right)\left(P_7^2 + P_8^2\right) + M_{32}P_7,$$
$$M_{38} = \frac{1}{16}M_{32}^2P_8 + \frac{1}{32}M_{32}Q_2\left(P_8^2 - P_7^2\right).$$

For the equations $X = X_0 + B_1X_1 + B_1^2X_2$, $Y = Y_0 + B_1Y_1 + B_1^2Y_2$, and $Z = Z_0 + B_1Z_1 + B_1^2Z_2$, we can obtain the corresponding graphical representations as follows,

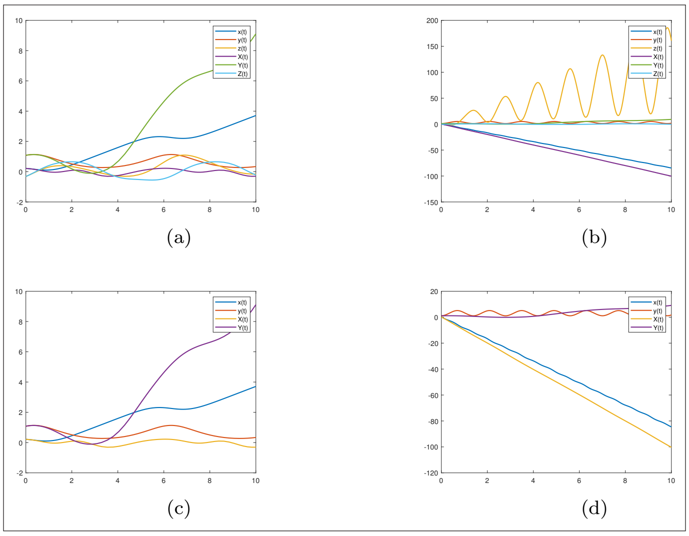

Figure 7: We compare the second-order solution (uppercase plots in Figure (a)) with the numerical solution (lowercase plots in Figure (a)). Considering the uncertainty in σt(where σ is constant), Figure (b) includes this term. For clarity, Figures (c) and (d) focus on ”x, X, y, Y”.

The performance of the first-order solution is notably superior to that of the second-order solution.

Magnetic Trajectory by the Fourth Killing Vector Field

The fourth instance of the Killing magnetic curve is described as:

$$\begin{cases} \ddot{x} + \dot{y}\left(\dot{z} + \frac{y}{2}\dot{x} - \frac{x}{2}\dot{y}\right) = -\dot{y}, \\ \ddot{y} - \dot{x}\left(\dot{z} + \frac{y}{2}\dot{x} - \frac{x}{2}\dot{y}\right) = \dot{x}, \\ \ddot{z} + \frac{y}{2}\ddot{x} - \frac{x}{2}\ddot{y} = 0. \end{cases} \tag{24}$$

A straightforward integration is feasible for the third equation:

$$\dot{z} + \frac{y}{2}\dot{x} - \frac{x}{2}\dot{y} = q.$$

By utilizing the expression in the initial and subsequent equations delineated in (24), we derive the resultant:

$$\dot{x} = p_1 \sin(t), \ \dot{y} = p_1 \cos(t).$$

We then employ these two expressions, multiply them by z, and subsequently perform the integration process to attain the desired result

$$\begin{cases} x = -p_1 \cos(t) + p_2, \\ y = p_1 \sin(t) + p_3, \\ z = \frac{1}{2}p_1 p_2 \sin(t) + \frac{1}{2}p_1 p_3 \cos(t) - \left(2 + \frac{p_1^2}{2}\right)t + p_4. \end{cases}$$

Conclusion

In this research, to obtain numerical solutions for the magnetic force curve in Heisen- berg space, we employ three different perturbation methods—the straightforward perturbation method, the Lindstedt−Poincare´ method, and the homotopy perturbation method—to calculate magnetic trajectories. Through graphical comparisons of their approximations, we conclude that the homotopy perturbation method offers the highest accuracy among the three [17-23].

Acknowledgments

We would like to extend our heartfelt gratitude to the anonymous referee for their invaluable feedback and profoundly insightful comments.

References

1. T de F Neves, Dalarme NB, Morais da Silva PM, Richard Landers, Carolina Siqueira Franco Picone, et al. (2020) Novel magnetic chi- tosan/quaternary ammonium salt graphene oxide composite applied to dye removal. J Environ Chemical Eng 8: 103820.
2. Farzin A, Etesami SA, Quint J, Adnan Memic, Ali Tamayol, et al. (2020) Magnetic nanoparticles in cancer therapy and diagnosis. Adv Healthcare Mater 9: 1901058.
3. Bejan CL, Binh TQ, Druta SL-Romaniuc (2023) Magnetic Frenet curves on para-Sasakian manifolds. Filomat 37: 1479-1496.
4. Calvaruso G, Munteanu MI, Perrone A (2015) Killing magnetic curves in three- dimensional almost paracontact manifolds. J Math Anal Appl 426: 423-439.
5. Munteanu MI, Nistor AI (2022) Magnetic curves in the generalized Heisenberg group. Nonlinear Analysis 214: 112571.
6. Korpinar T, Bas S (2019) A new approach for inextensible flows of binormal spherical indicatrices of magnetic curves. Int J Geom Methods Mod Phys 16: 1950020.
7. Lee JE (2019) Slant curves and contact magnetic curves in Sasakian Lorentzian 3- manifolds. Symmetry 11: 784.
8. Erjavec Z (2019) On killing magnetic curves in SL (2, R) geometry. Rep Math Phys 84: 333-350.
9. Inoguchi J, Munteanu MI (2023) Killing submersions and magnetic curves. J Math Anal Appl 520: 126889.
10. Sun J (2020) Singularity properties of null killing magnetic curves in Minkowski 3-space. Int J Geom Methods Mod Phys 17: 2050141.
11. Kelekci O,, Du¨ndar F S, Ayar G (2024) Classification of Killing magnetic curves in H3. International Journal of Geometric Methods in Modern Physics 20: 2450006.
12. Nayfeh AH (1993) Introduction to Perturbation Techniques. Wiley, New York https://download.e-bookshelf.de/download/0000/6033/50/L-G-0000603350-0002365185.pdf.
13. J-H He (1999) Homotopy perturbation technique. Computer Methods in Applied Mechanics and Engineering 178: 257-262.
14. Breton N, Lammerzahl C, Macias A (2022) Rotating structure of the Euler- Heisenberg black hole. Phys Rev D 105: 104046.
15. Bakopoulos A, Thanasis Karakasis, Nick E Mavromatos, Theodoros Nakas, Eleftherios Papantonopoulos, et al. (2024) Exact black holes in string-inspired Euler-Heisenberg theory. Phys Rev D 110: 024014.
16. Kordyukov Y, Sukochev F, Zanin D (2024) Principal symbol calculus on contact mani- folds. Lecture Notes in Mathematics https://link.springer.com/book/10.1007/978-3-031-69926-9.
17. Blair DE (2010) Riemannian Geometry of Contact and Symplectic Manifolds. Progress in Mathematics https://link.springer.com/book/10.1007/978-0-8176-4959-3.
18. Jleli M, Munteanu IM, Nistor IA (2015) Magnetic trajectories in an almost contact metric manifold R2N +1. Results in Mathematics 67: 125-134.
19. Rahmani N, Rahmani S (2006) Lorentzian geometry of the Heisenberg group. Geometriae Dedicata 118: 133-140.
20. Jazar RN (2021) Perturbation Methods in Science and Engineering. Springer https://link.springer.com/book/10.1007/978-3-030-73462-6.
21. Liu GL (1997) New research directions in singular perturbation theory: artificial parameter approach and inverse-perturbation technique. Proceedings of the 7th Conference on Modern Mathematics and Mechanics, Shanghai 47-53.
22. Liao SJ (1997) Boundary element method for general nonlinear differential operators. Eng Anal Bound Elements 20: 91-99.
23. He JH (2003) Homotopy perturbation method: a new nonlinear analytical technique. Applied Mathematics and Computation 135: 73-79.